Technical Report

TR-10-30

Thermodynamic properties of copper compounds with oxygen and hydrogen from first principles

P A Korzhavyi, B Johansson
Applied Materials Physics
Department of Materials Science and Engineering
Royal Institute of Technology

February 2010

Svensk Kärnbränslehantering AB
Swedish Nuclear Fuel
and Waste Management Co

Box 250, SE-101 24 Stockholm
Phone +46 8 459 84 00

Thermodynamic properties of copper compounds with oxygen and hydrogen from first principles

P A Korzhavyi, B Johansson
Applied Materials Physics
Department of Materials Science and Engineering
Royal Institute of Technology

February 2010

Abstract

We employ quantum-mechanical calculations (based on density functional theory and linear response theory) in order to test the mechanical and chemical stability of several solid-state configurations of Cu^{1+}, Cu^{2+}, O^{2-}, H^{1-}, and H^{1+} ions. We begin our analysis with cuprous oxide (Cu_2O, cuprite structure), cupric oxide (CuO, tenorite structure), and cuprous hydride (CuH, wurtzite and sphalerite structures) whose thermodynamic properties have been studied experimentally. In our calculations, all these compounds are found to be mechanically stable configurations. Their formation energies calculated at $T = 0$ K (including the energy of zero-point and thermal motion of the ions) and at room temperature are in good agreement with existing thermodynamic data. A search for other possible solid-state conformations of copper, hydrogen, and oxygen ions is then performed. Several candidate structures for solid phases of cuprous oxy-hydride (Cu_4H_2O) and cupric hydride (CuH_2) have been considered but found to be dynamically unstable. Cuprous oxy-hydride is found to be energetically unstable with respect to decomposition onto cuprous oxide and cuprous hydride. Metastability of cuprous hydroxide (CuOH) is established in our calculations. The free energy of CuOH is calculated to be some 50 kJ/mol higher than the average of the free energies of Cu_2O and water. Thus, cuprite Cu_2O is the most stable of the examined Cu(I) compounds.

Introduction

Szakálos *et al.* /1/ have reported corrosion of copper, accompanied by evolution of hydrogen gas, to occur spontaneously in pure, de-ionized, O_2-free water at 73°C. These new observations continue the series of experimental studies by Hultquist *et al.* /2, 3, 4/ which claim corrosion of copper by pure water. The results of these studies have been repeatedly criticized /5, 6/ as inconsistent with basic thermodynamic data on the copper-oxygen-hydrogen system /7, 8, 9, 10/ on which the design of copper canisters for nuclear waste storage is based /11, 12, 13/.

In order to explain the observed hydrogen evolution, Szakálos *et al.* /1/ had to postulate the existence of a previously unknown phase, copper oxy-hydride CuH_xO_y ($x \approx y \leq 1$), so stable that it can decompose water. X-ray diffraction off the corrosion products formed on copper did not reveal any new structure, so the authors of Ref. /1/ concluded that the oxy-hydride phase could be structurally described as "protonated" cupric or cuprous oxide, CuH_xO_1 or $CuH_xO_{0.5}$, respectively. The well-known thermodynamic stability of hydrogen-free oxides of copper is not enough to decompose water.

At the oxygen-free end of composition for the hypothetical corrosion product one has a highly unstable compound, copper(I) hydride CuH. This poorly crystalline compound /14/ belongs to the family of so-called polymeric hydrides. It is thermodynamically unstable /15, 16/, even with respect to elemental Cu and H_2, but is metastable in the presence of water, so that CuH can be formed chemically or electrochemically in aqueous media /17, 18, 19/. Intermediate compounds between the oxides and the hydride of copper (oxy-hydrides), as well as their thermodynamic properties, are presently unknown. Copper(II) hydroxide $Cu(OH)_2$ is known to be metastable; it spontaneously decomposes onto CuO and water. Copper(I) hydroxide, CuOH, exists in molecular form (also as neutral molecular species in aqueous solution /13/), but is not known to exist as a solid phase.

Contents

1 Methodology

In the present study, we derive the thermodynamic properties of copper oxy-hydrides theoretically, using first-principles calculations of the electronic structure and phonon spectra for the oxides, hydrides, and oxy-hydrides of copper. The present electronic structure calculations are based on density functional theory /20, 21/, and employ the generalized gradient approximation (GGA) /21/. Ultra-soft pseudopotentials /22/ and the plane-wave self-consistent-field (PWscf) code /23/ are used in order to calculate the total energy as a function of nuclear positions.

In cases of systems containing light elements, the total energies obtained as a result of DFT calculations are insufficient for deriving thermodynamic information even at $T = 0$ K, because they do not include the energy of zero-point motion of the nuclei. The zero-point energy (ZPE) scales as $M^{-1/2}$, where M is the nuclear mass, and cannot be neglected for light atoms such as hydrogen. Therefore, we calculate the energy of zero-point motion and include it in the present thermodynamic analysis of all the studied phases. Next, we perform a thermodynamic integration of the calculated phonon densities of states, in order to extend the results from zero temperature to finite temperatures. For solid phases (pure copper, copper oxides, copper hydride, and copper oxy-hydrides) the phonon spectra are calculated using the linear-response technique /24/, as implemented within the program package PHONON of the Quantum Espresso /25/ distribution. For diatomic gaseous species (O_2, H_2, Cu_2, and CuH) the dimer energy is calculated as a function of internuclear distance and then used as the effective potential in quantum-mechanical calculations of the equilibrium bond length, bond strength, and zero-point energy of the molecules /26/. The relatively small rotational energy contributions are neglected in the zero-point energy calculations, but are included in the finite-temperature analysis. For this purpose, we use tabulated data /27/ for diatomic molecules (the data contain the rotational contribution as well as all the other necessary contributions).

Using a thermodynamic integration of the calculated phonon spectra, one can obtain free energy, heat capacity, and entropy for each phase as a function of temperature. However, as we will see below, the phonon spectra for many of the considered solid-state structures of copper hydrides and oxy-hydride contain imaginary frequencies, so that a thermodynamic integration (which is made possible by setting all the imaginary modes to zero frequency) is not very accurate in these cases. However, the magnitude of finite-temperature contributions to energy is small on the scale of the enthalpy of formation in such cases, so that an analysis at $T = 0$ K is sufficient for the purpose of the present study. Accurate experimental data exist /16, 27/ on the heat capacities for all the substances that our calculations predict to be dynamically stable (i.e., to have all real vibrational frequencies).

We consider three states of ionic motion: a hypothetical state in which the ions are static (as usual in electron-structure calculations), another state that corresponds to $T = 0$ (i.e. includes zero-point motion of the ions), and finally the system is considered at room temperature $T = 298.15$ K (thermal motion is added). Standard states for the elements are chosen to be in the same state of ionic motion (i.e., at the same ionic temperature). As the standard states we consider face-centered-cubic (fcc) copper (a mixture of ^{63}Cu and ^{65}Cu isotopes with an average atomic mass 63.55), hydrogen gas $^1H_2$ (singlet state $^1\Sigma_g^+$), and oxygen gas $^{16}O_2$ (triplet state $^3\Sigma_g^-$). At $T = 0$ the reference energy E_0 (or enthalpy H_0) for each of these species contains two contributions, the total energy for static ions U_0 and the zero-point energy ZPE,

$$E_0 = U_0 + \mathrm{ZPE} \tag{1-1}$$

The energy of formation for a (meta)stable compound $Cu_kH_lO_m$ ($k + l + m = N$) is calculated as

$$\Delta E_0(\mathrm{Cu}_k\mathrm{H}_l\mathrm{O}_m) = E_0(\mathrm{Cu}_k\mathrm{H}_l\mathrm{O}_m) - \frac{k}{N}E_0(\mathrm{Cu}) - \frac{l}{2N}E_0(\mathrm{H}_2) - \frac{m}{2N}E_0(\mathrm{O}_2) \tag{1-2}$$

whereas for dynamically unstable substances (for which, strictly speaking, ZPE cannot be defined) we mainly use total energies uncorrected for zero-point ionic motion:

$$\Delta U_0(\mathrm{Cu}_k\mathrm{H}_l\mathrm{O}_m) = U_0(\mathrm{Cu}_k\mathrm{H}_l\mathrm{O}_m) - \frac{k}{N}U_0(\mathrm{Cu}) - \frac{l}{2N}U_0(\mathrm{H}_2) - \frac{m}{2N}U_0(\mathrm{O}_2) \tag{1-3}$$

A finite-temperature thermodynamic integration of the phonon density of states $g(\omega)$ has been performed using the standard formalism of quasi-harmonic approximation. Zero-point energy is first added to the electronic-structure energy U_0 to obtain the total energy at $T = 0$ K.

$$E_0 = U_0 + \frac{1}{2}\int_0^\infty \hbar\omega \cdot g(\omega) d\omega \tag{1-4}$$

Total energy at a finite temperature, $E(T)$, is given by

$$E(T) = E_0 + \int_0^\infty \frac{\hbar\omega \cdot g(\omega) d\omega}{\exp(\hbar\omega / k_B T) - 1} \tag{1-5}$$

Heat capacity at a constant volume V, C_V, has been obtained as

$$C_V = k_B \int_0^\infty \left(\frac{\hbar\omega}{2k_B T} \right)^2 \frac{g(\omega) d\omega}{\sinh^2(\hbar\omega / 2k_B T)} \tag{1-6}$$

Helmholtz free energy is finally calculated as

$$F(T) = U_0 + k_B T \int_0^\infty \ln\left[2\sinh\left(\hbar\omega / 2k_B T\right)\right] d\omega \tag{1-7}$$

In order to include anharmonic effects, such as thermal expansion, the procedure is repeated at several volumes around the energy minimum of $U_0(V)$. This gives one the access to pressure, enthalpy, Gibbs free energy, and heat capacity C_P, all at a constant pressure P (in the present study, we are interested in the data corresponding to $P = 0$).

2 Results

2.1 Molecular species

In order to calculate the reference energies for the gaseous species, as well as to test several available pseudopotentials, we studied the vibrational properties of $^{1}H_2$, $^{16}O_2$, $^{63}Cu_2$, and $^{63}Cu^{1}H$ dimer molecules. Each dimer was considered in an otherwise empty simulation box (16×16×16 bohr); the total energy was calculated as a function of the internuclear distance r in the molecule. The calculation results are presented in Figure 2-1. The dependence was then fitted by the Morse potential function:

$$U(r) = C + D\left[\exp\left(-2\alpha\frac{r-r_0}{r_0}\right) - 2\exp\left(-\alpha\frac{r-r_0}{r_0}\right)\right] \quad (2\text{-}1)$$

The results of the fit are shown in Figure 2-1 as lines. The Schrödinger equation for ionic motion in the potential $U(r)$ can be solved analytically and its energy spectrum has the following form:

$$E = C - D + \hbar\omega_0\left(n+\frac{1}{2}\right) - \hbar\cdot x\omega_0\left(n+\frac{1}{2}\right)^2 \quad (2\text{-}2)$$

where ω_0 and $x\omega_0$ are the harmonic frequency and the first anharmonicity parameter, respectively, and n is the vibrational main quantum number which can take non-negative integer values. Vibrational contribution, which is the largest part of the zero-point energy, may approximately be expressed as:

$$\mathrm{ZPE} \approx \frac{1}{2}\hbar\omega_0 - \frac{1}{4}\hbar\cdot x\omega_0 \quad (2\text{-}3)$$

Table 2-1 shows the calculated zero-point energy for the considered dimer molecules; the calculated data are compared with recent spectroscopic data. The comparison shows that the simple approximation given by Eq. (2-3) is rather accurate, because the vibrational frequencies are typically much higher than the rotational frequencies for the same species. However, rotational degrees of freedom are the first to be excited at nonzero temperatures, and, therefore, to contribute to the heat capacity. In the present study, we do not perform calculations for rotational and other effects in molecules, but take the results of previous careful calculations published in the form of thermodynamic tables /27/ for the gaseous species (H_2 and O_2 molecules are of interest for the present study).

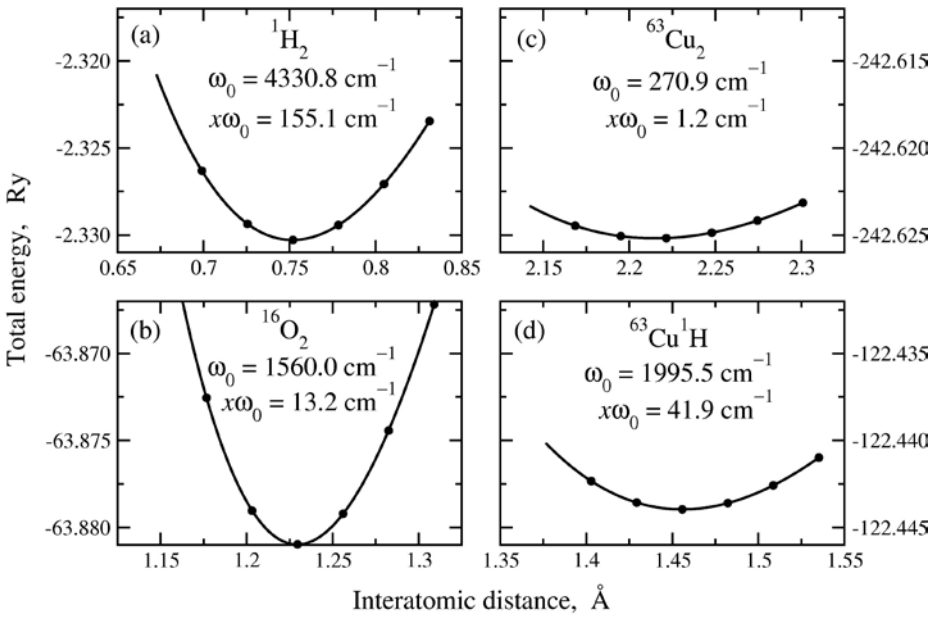

Figure 2-1. *Calculated dependencies of total energy on the internuclear distance in dimer molecules H_2, O_2, Cu_2 and CuH. For each dimer, numerical values are given to the potential parameters defined by Eq. (2-2).*

Table 2-1. Calculated parameters of vibrational motion for dimer molecules $^{1}H_2$, $^{16}O_2$, $^{63}Cu_2$, and $^{63}Cu^{1}H$: the characteristic bond length r_0 (Å), the eigenfrequency ω_0 (cm^{-1}), the first anharmonicity parameter $x\omega_0$ (cm^{-1}), and the zero-point energy ZPE (cm^{-1}). Corresponding experimental values are given for comparison.

Dimer	Source	r_0	ω_0	$x\omega_0$	ZPE
$^{1}H_2$	This work	0.7517	4,330.76	155.14	2,126.59
	Ref./26/	0.7414	4,401.21	121.34	2,179.30
$^{16}O_2$	This work	1.2294	1,560.09	13.22	776.74
	Ref./26/	1.2075	1,580.19	11.98	787.38
$^{63}Cu_2$	This work	2.2149	264.55	1.02	135.14
	Ref./26/	2.2197	270.89	1.21	–
$^{63}Cu^{1}H$	This work	1.4557	1,941.26	37.51	987.30
	Ref./26/	1.4626	1,995.54	41.90	–

2.2 Copper oxides and hydrides

We have performed calculations for Cu_2O (cuprite structure), and CuH (wurtzite and sphalerite structures) according to the scheme outlined in Sec. 1. Figure 2-2 shows that these compounds are semiconductors; the calculated bandgaps are very similar. Since the experimental bandgap of Cu_2O (about 2 eV) is underestimated in the LDA-based calculations, the same may be expected for CuH.

Some of the calculated phonon spectra of Cu_2O and CuH(wurtzite) are presented in Figures 2.3–2.6 for different volumes. Because of the structural similarity between wurtzite and sphalerite, the phonon spectra of CuH(sphalerite) look very similar to those of CuH(wurtzite) and, therefore, the former are not shown. There is a certain similarity between the phonon spectra of Cu_2O and CuH: they all have a frequency gap between the high-frequency optical modes [which are due to the light elements (O or H)] and the low-lying acoustic modes and optical Cu modes. The discontinuity near point Γ seen in Figures 2-5 and 2-6 for high-lying optical modes is due to polarity of the CuH(wurtzite) structure (so-called LO – TO splitting of longitudinal and transverse optical modes in polar dielectric crystals).

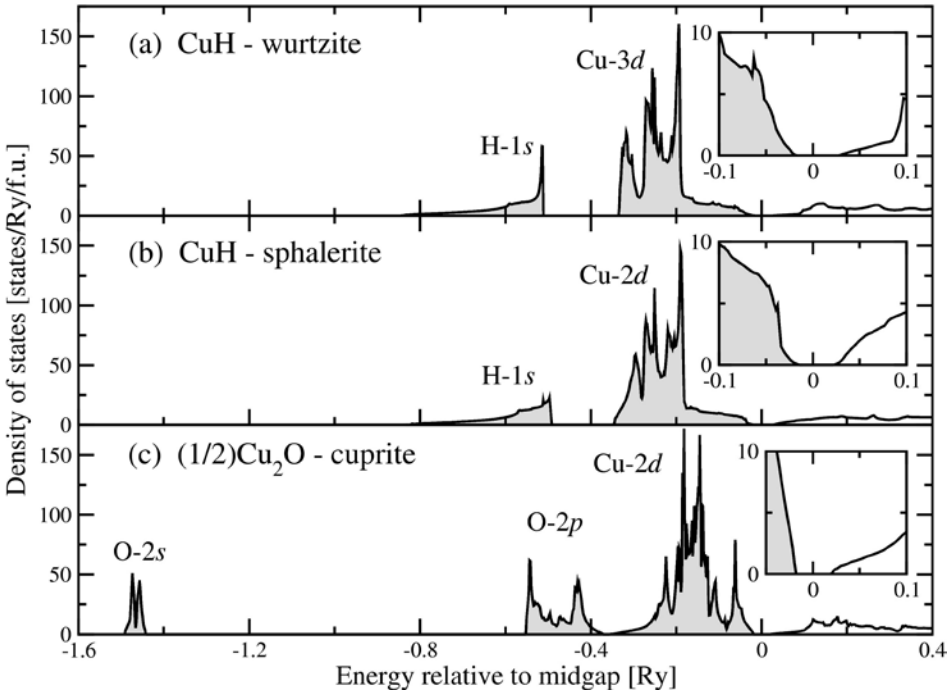

Figure 2-2. *Density of electron states (DOS) in copper hydride, CuH, and cuprous oxide, Cu_2O. Labels near the DOS peaks indicate the predominant character of the corresponding states. The insert panels magnify the DOS at energies near the bandgap.*

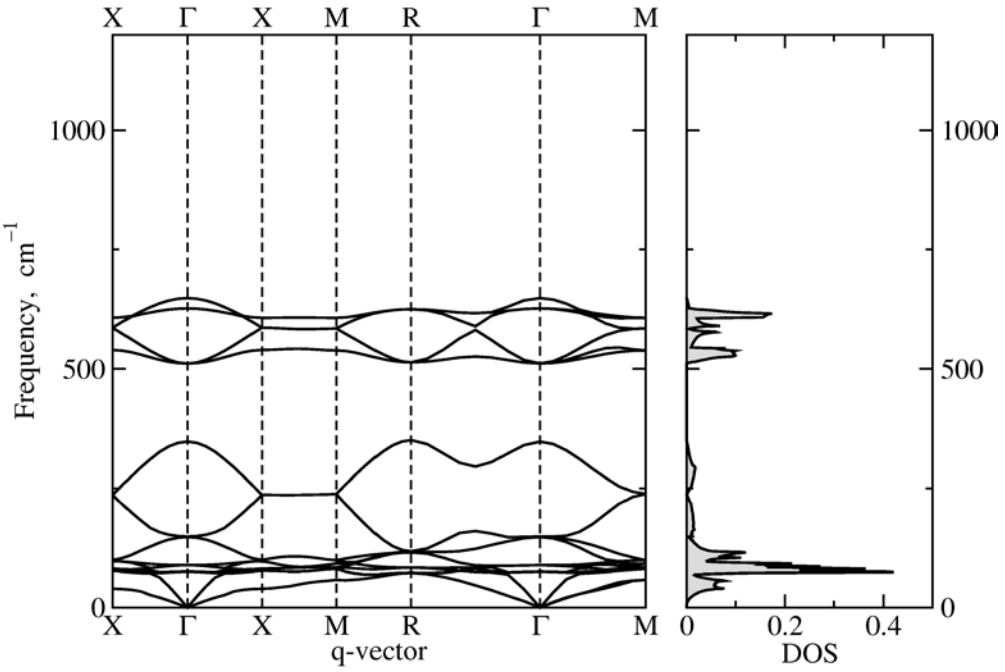

Figure 2-3. *Phonon spectrum and density of states (DOS) in cuprous oxide, Cu_2O, calculated at the lattice parameter a = 4.286 Å.*

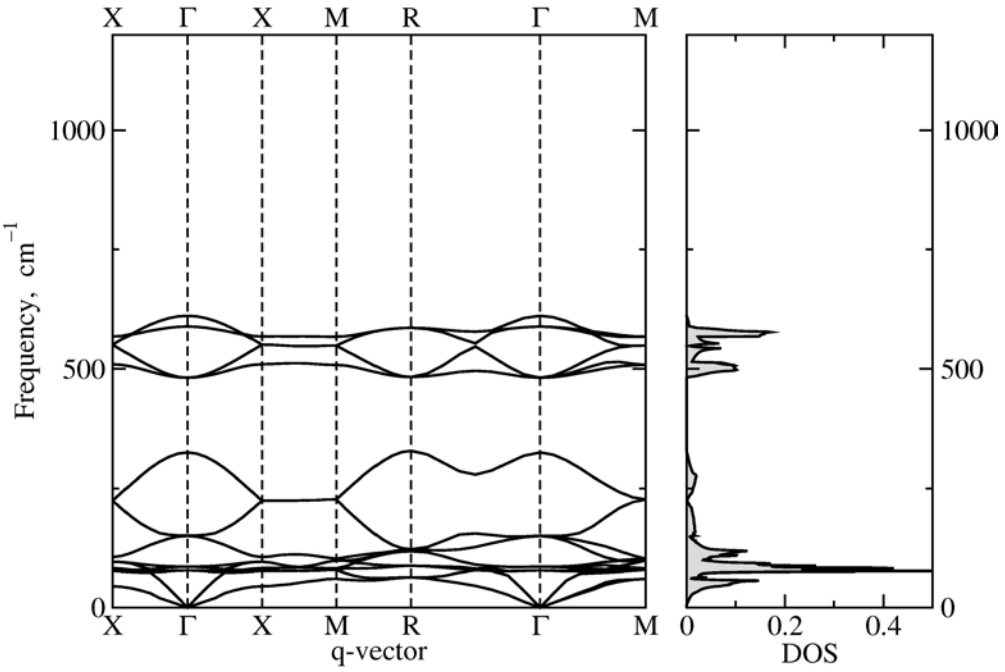

Figure 2-4. *Phonon spectrum and density of states (DOS) in cuprous oxide, Cu_2O, calculated at the lattice parameter a = 4.339 Å.*

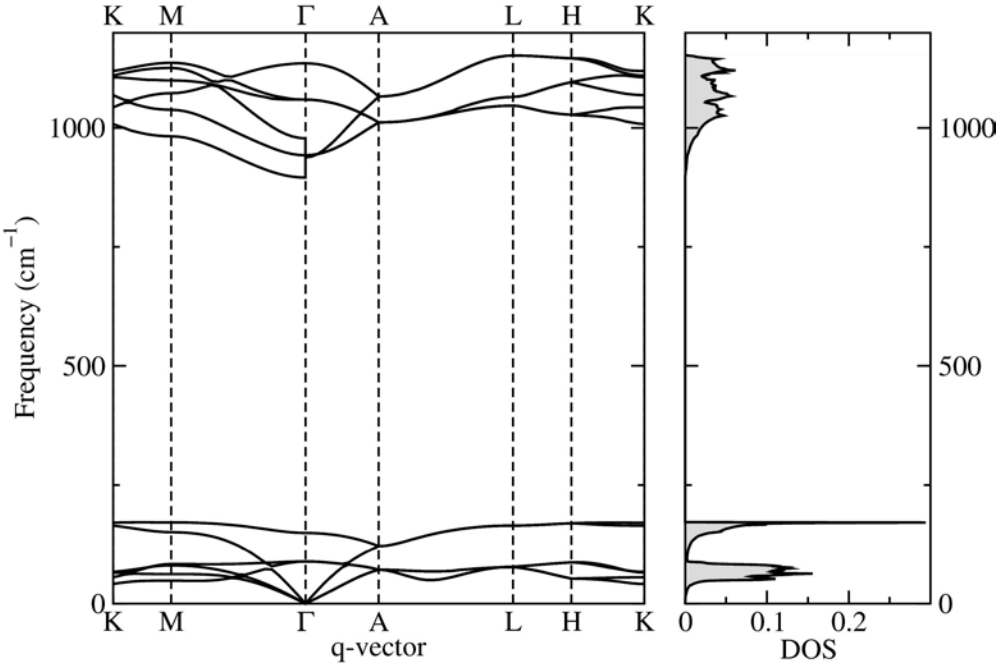

Figure 2-5. *Phonon spectrum and density of states (DOS) in copper hydride, CuH(wurtzite), calculated at the lattice parameter a = 2.866 Å.*

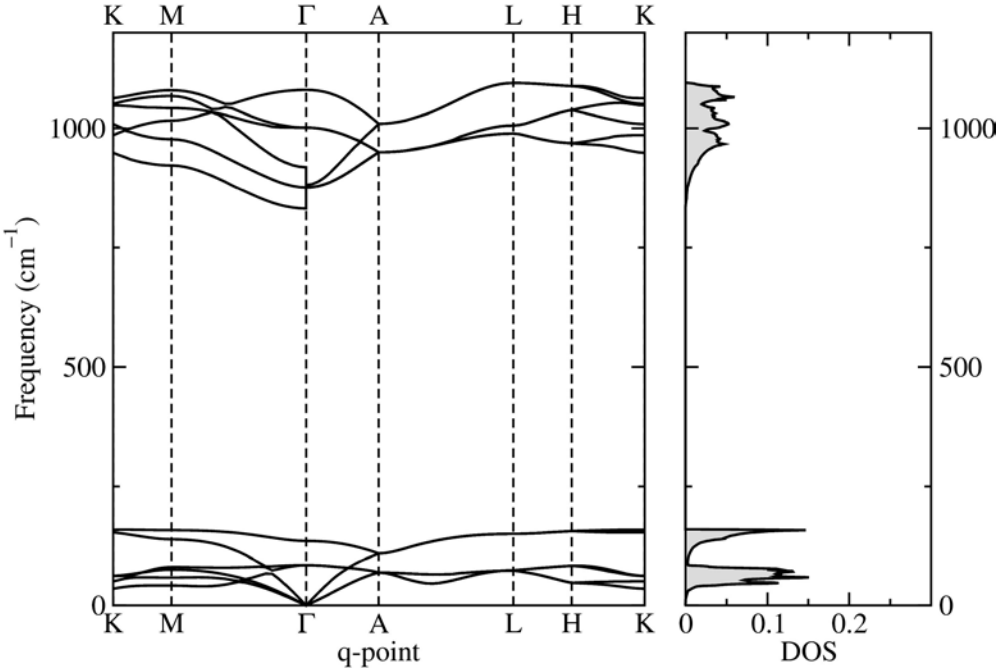

Figure 2-6. *Phonon spectrum and density of states (DOS) in copper hydride, CuH(wurtzite), calculated at the lattice parameter a = 2.904 Å.*

The presence of a wide gap in the phonon spectrum, between low- and high-frequency modes, alters the shape of the corresponding heat-capacity curves (see Figures 2-7 and 2-8). We note from the figures that the linear response theory can describe the shapes of the C_P curves of copper oxides and hydrides very accurately, especially at low temperatures.

Using a thermodynamic integration of the calculated vibrational spectra, we have obtained the thermal properties of the considered solids; some examples are shown in Figure 2-9. Cuprite Cu_2O is known to have a low value of thermal expansion coefficient around room temperature, and to exhibit a negative thermal-expansion behavior at low temperatures. Qualitatively, this anomalous behavior is captured by our calculations.

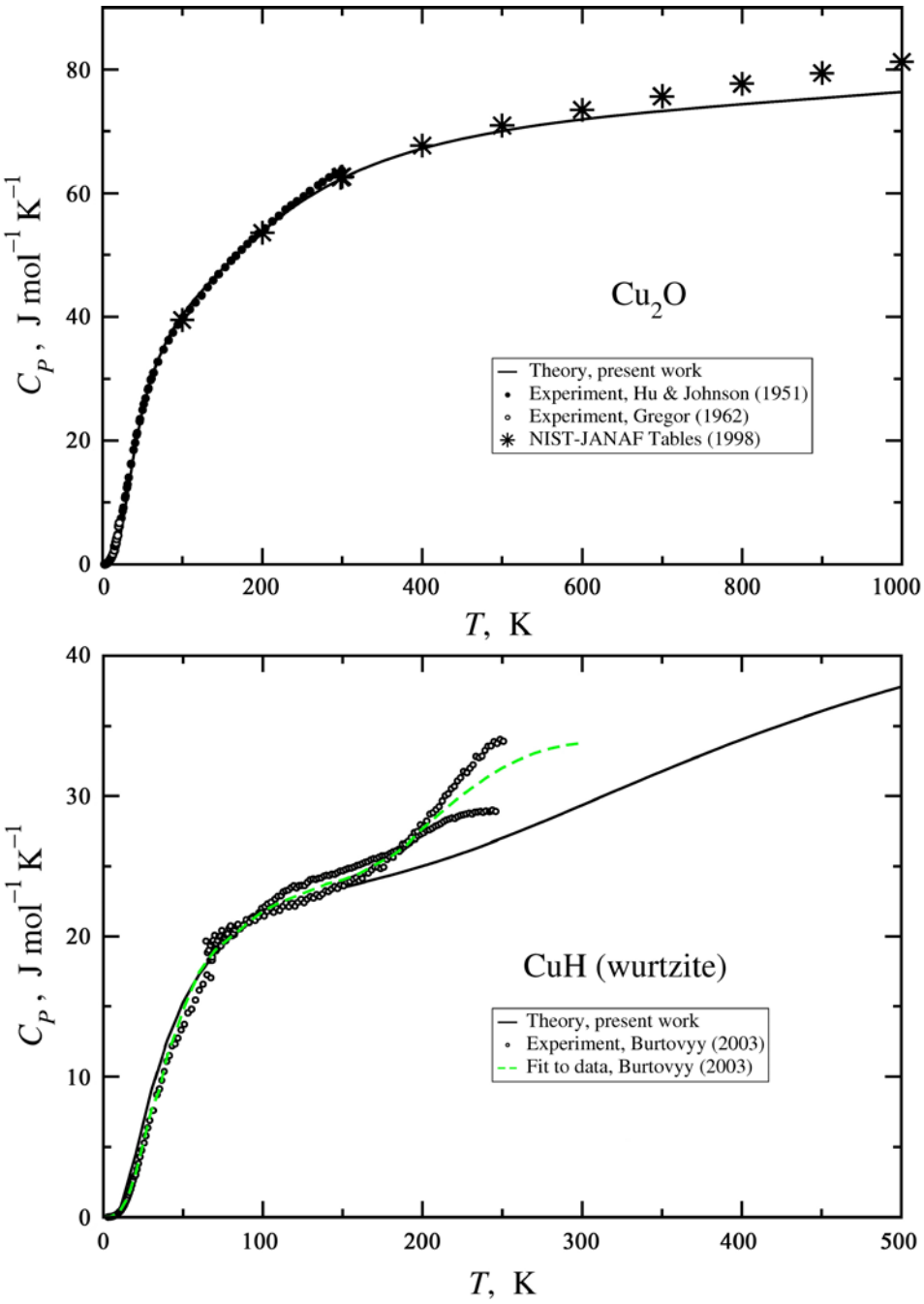

Figure 2-7. *Calculated and experimental heat capacities C_P of Cu_2O (upper panel) and CuH wurtzite (lower panel).*

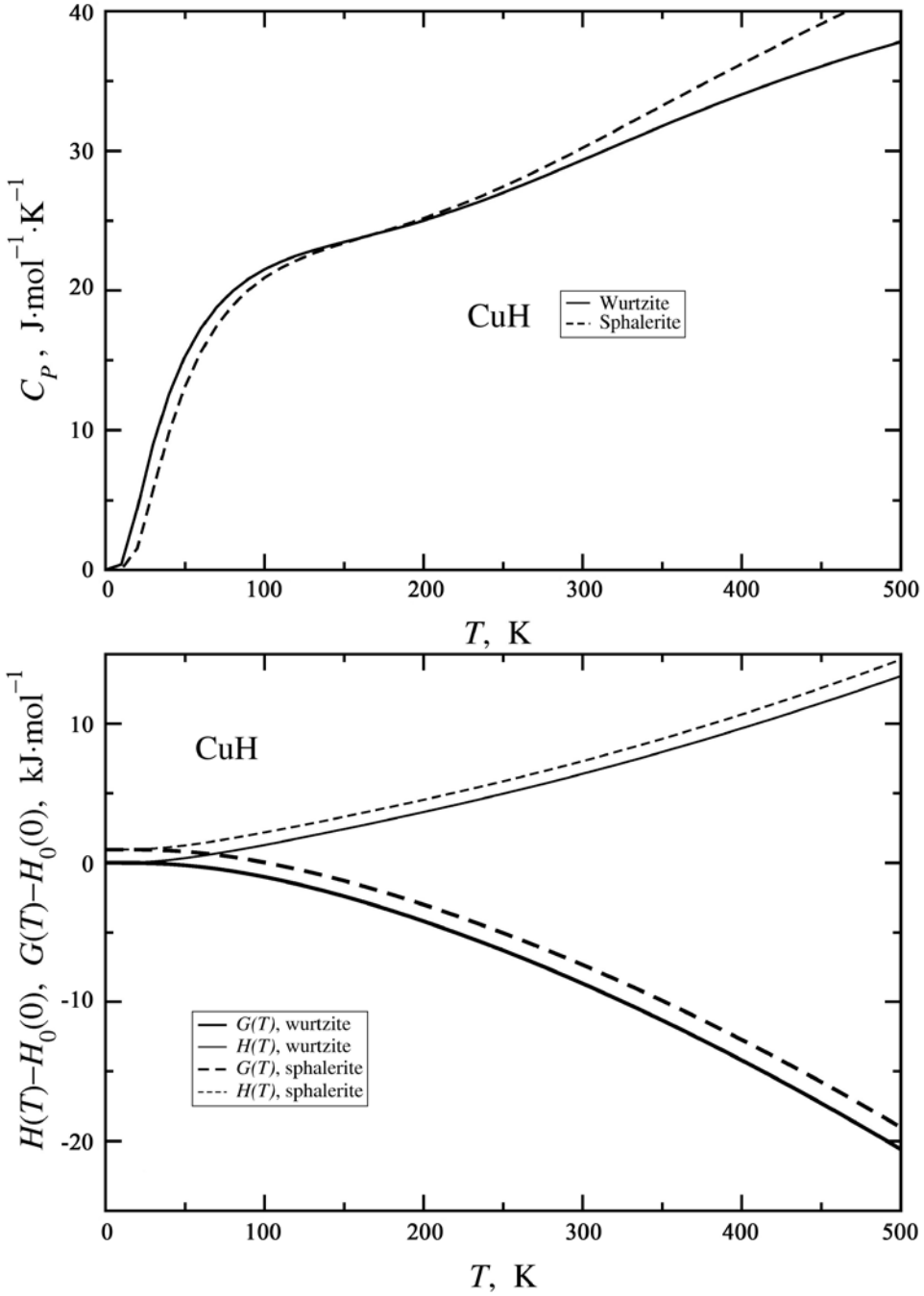

Figure 2-8. *Calculated heat capacities (upper panel) and enthalpies (lower panel) for both the wurtzite and sphalerite crystal structures of CuH.*

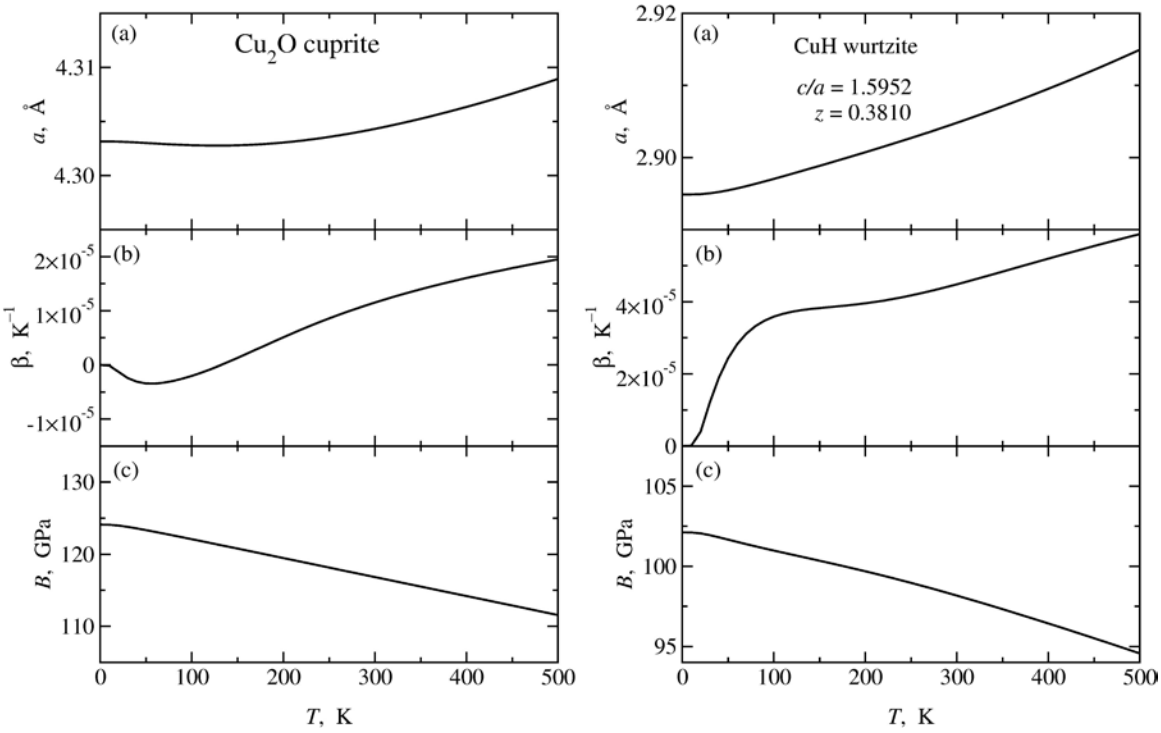

Figure 2-9. *Calculated temperature dependencies of the physical properties of Cu_2O (left panel) and CuH wurtzite (right panel): lattice parameter a, thermal (volume) expansion coefficient β, and bulk modulus B. Note that our calculations qualitatively reproduce the low-temperature thermal expansion anomaly in Cu_2O. CuH is predicted to have no such anomaly.*

Negative thermal expansion is characteristic of materials whose structure contains relatively long chains of atoms. The frequencies of transverse vibrations of such chains are typically rather low when the chain is relaxed, but the frequencies increase the chain is stretched, similar to the tune of a guitar string. All other frequencies (corresponding to three-dimensional, "bulky" atomic configurations) typically *decrease upon expansion*. However, the frequencies of transverse vibrational modes for the quasi-one-dimensional atomic chains (these modes have low frequencies) *decrease upon compression*. For such anomalous modes, which can easily be identified by comparing Figures 2-3 and 2-4, the so-called mode Grüneisen parameter $\gamma = -d\ln\omega / d\ln V$ will be negative (normally it is positive). Therefore, at low temperatures, the structure will gain some additional vibrational entropy by shrinking the volume so that the chains become lose and the corresponding frequencies decrease. When the temperature is increased above a certain threshold, so that higher-lying modes are excited whose frequencies decrease upon expansion, the thermal expansion behavior will return to normal.

Cu_2O is not unique in showing thermal expansion anomaly; an even stronger anomaly is exhibited by Ag_2O (also the cuprite crystal structure, with linearly coordinated cations). Rubber and some other polymeric materials have negative thermal expansion coefficients, due to the fact that their structures consist of long and flexible molecular chains. Negative thermal expansion behavior has also been reported to occur at low temperatures in cubic semiconductors (Si, Ge, GaAs, and AlAs) having open structures. This anomalous behavior is also attributed to negative mode Grüneisen constants for some zone-boundary acoustic phonons.

The wurtzite structure of CuH has a tetrahedral coordination of cations and anions; it shows no thermal expansion anomaly, despite the fact that it is a semiconductor. Also, there are structural similarities between Cu_2O and CuH: they both have a close-packed cation sublattice with the anions occupying tetrahedral intersites. Figure 2-8 shows that the hexagonal and cubic forms of CuH are very close in energy (polytypism). The hexagonal (wurtzite) structure of CuH is predicted to be lower in energy than the cubic (sphalerite) structure in the whole temperature range of metastability of copper hydride, from 0 K to about 330 K. This result agrees with experimental observations.

Therefore, in the following search for stable or metastable configurations of copper oxy-hydride, we adopt the following structural model: we assume that its structure may be derived from the close-packed cation sublattice with the anions (O^{2-} and H^- species) distributed among the tetrahedral interstitial sites so that they do not occur too close to one another in the structure. Naturally, the charged O^{2-} species repel each other and therefore cannot occur closely. If an O^{2-} and a H^- occur too close, hydrogen may recharge (minus to plus) to form a hydroxyl ion OH^-. Then the substance may no longer be described as an oxy-hydride.

Before discussing the search procedure in more details, let us analyze the enthalpy and free energy balance for the substances for which experimental data are available. The results of thermodynamic integration, based entirely on calculations (as well as on calculated and tabulated /27/ data for the H_2 and O_2 molecules) are summarized in Table 2-3. Raw data on total energies are collected in Table 2-2.

A straightforward calculation of the enthalpy of formation yields a value of about −113 kJ/mol, in good agreement with the value −120 kJ/mol obtained by Soon *et al.* using GGA-based first-principles calculations /28, 29, 30, 31/, but which is much less negative than the experimental value −169 kJ/mol /27/. This big mismatch is quite unexpected because, as discussed above, the other cohesive properties of the oxide are described very accurately.

The problem here stems from the well-known fact that stability of small molecules is not accurately reproduced by the existing density-functional approximations (including the GGA). Thus, the stability of an O_2 dimer is *overestimated* by 1.01 eV whereas the stability of an H_2 dimer is *underestimated* by 0.21 eV /32/. Molecular oxygen represents the hardest case for density functional theory.

However, since the experimental atomization energies are accurately known /27/, the problem may be completely eliminated by correcting the calculated energies of O_2 and H_2 molecules (listed in Table 2-2) by the amount of error known from molecular tests /32/, i.e. by +0.074 Ry and −0.016 Ry, respectively. One can see from Table 2-3 below that, by shifting the total energy of the oxygen and hydrogen molecules, one recovers good agreement between calculations and experiment, for both cupric and cuprous oxide, at all temperatures. In the following, we apply this correction to all considered copper-oxygen-hydrogen compounds.

Table 2-2. Raw data for the thermodynamic stability analysis (results of thermodynamic integration of the electronic and ionic free energy contributions). All energies are in Rydberg atomic units (Ry/cell). Composition of the primitive cell for each substance is given in the second column (Structural unit).

Substance	Str. unit	U_0	$H(0)$	$H(298.15)$	$G(298.15)$
$^{1}H_2$	H_2	–2.330284	–2.310905	–2.304455	–2.334135
$^{16}O_2$	O_2	–63.880981	–63.873903	–63.867288	–63.913881
$^{63.55}$Cu(fcc)	Cu	–121.487552	–121.485440	–121.481626	–121.489158
Cu_2O	Cu_4O_2	–550.006667	–549.985388	–549.965494	–550.010147
CuO	Cu_2O_2	–307.008411	–306.992208	–306.980973	–307.002211
CuH wurtzite	Cu_2H_2	–245.268593	–245.237435	–245.227688	–245.250681
CuH_2 fluorite	CuH_2	–123.725675	–123.709162	–123.700968	–123.714541
CuH_2 rutile	CuH_2	–123.759402	–123.730836	–123.725195	–123.736886
Cu_4H_2O	Cnf.1	–520.180620	–	–	–
Cu_4H_2O	Cnf.2	–520.216655	–520.176862	–520.156605	–520.203153
Cu_4H_2O	Cnf.3	–520.228321	–520.189736	–520.170066	–520.212964

2.3 Oxy-hydrides and di-hydrides of copper

Taking into account the structural and chemical similarity between the cation sublattices in Cu_2O and CuH, we have checked the possibility that the O^{2-} and H^- anions may form an alloy within a common structural framework. We set up three initial configurations, starting from the unit cell of cuprite (Cu_4O_2). If one uses the setting where one oxygen is in the cube corners (0, 0, 0) and the other one is in the center (0.5, 0.5, 0.5), the coordinates of copper atoms are then (0.25, 0.25, 0.25), (0.75, 0.75, 0.25), (0.75, 0.25, 0.75), and (0.25, 0.75, 0.75). To create the oxy-hydride configurations, we removed the central oxygen atom and inserted two hydrogen atoms, thereby creating a charge-compensated substitution (attempting to get a semiconducting structure, which could be energetically favorable).

We tried the following three initial configurations (tetragonal structures), in which the two hydrogen atoms were put in the following positions:

Configuration 1: H(0.5, 0.5, 0.5), H(0.0, 0.0, 0.5);

Configuration 2: H(0.5, 0.5, 0.5), H(0.5, 0.5, 0.0);

Configuration 3: H(0.5, 0.0, 0.5), H(0.0, 0.5, 0.5).

After that, damped dynamics simulations were performed for the three initial configurations assuming a tetragonal symmetry of the simulation box (allowing the atoms to relax according to forces and the lattice parameters to adjust so that the stress tensor components become zero). Fully relaxed configurations were thereby attained. The value of the Gaussian broadening parameter (used for improving the convergence of k-space integrals) was found to slightly affect the relaxation process, producing slightly different relaxed structures at different values of the parameter. Configurations 2 and 3 have been obtained by performing the damped dynamics relaxation under the Gaussian broadening parameter of 0.02 Ry. Relaxation of Configuration 1 was later abandoned due to the too high energy of this as compared to the other configurations. All the configurations were found to be metallic rather than semiconducting.

In addition, we calculated the electronic and phonon structures of copper di-hydride (cupric hydride) CuH_2, which was considered in the fluorite and rutile crystal structures. The structures were fully relaxed prior to phonon spectra calculations.

Even after the full relaxation, all the considered Cu_4H_2O and CuH_2 configurations were found to be dynamically unstable. Their phonon spectra were found to exhibit imaginary frequencies some vibrational modes (the phonon spectrum for fully relaxed Configuration 3 of Cu_4H_2O is shown in Figure 2-10 as an example). The resulting dynamical instability is rather weak, but it is additional evidence that these compounds are not really “healthy”, since the atoms cannot really hold together.

Nevertheless, we used the calculated total energies and phonon spectra of Configurations 2 and 3 of Cu_4H_2O (with the imaginary frequencies set to zero) in order to evaluate the thermodynamic stability of copper oxy-hydride. The results are summarized in Table 2-3.

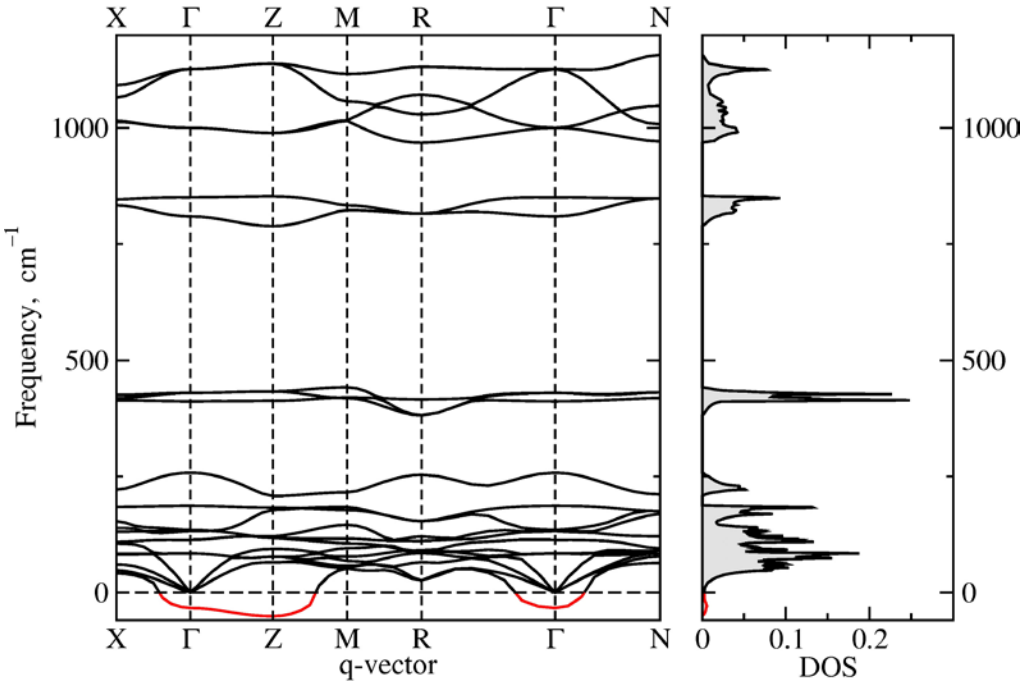

Figure 2-10. Phonon spectrum and density of states (DOS) in copper oxy-hydride Cu_4H_2O in the fully-relaxed atomic Configuration 3, with the lattice parameters a = 4.225 Å and c = 3.821 Å (c/a = 0.904).

The notations for q-vectors are as follows: $\Gamma = \frac{\pi}{a}(0, 0, 0)$; $X = \frac{\pi}{a}(1, 0, 0)$; $Z = \frac{\pi}{a}(0, 0, a/c)$;

$M = \frac{\pi}{a}(0, 1, a/c)$; $R = \frac{\pi}{a}(1, 1, a/c)$; $N = \frac{\pi}{a}(1, 1, 0)$.

Imaginary phonon frequencies are shown as negative values and indicated by red color.

Table 2-3. Estimated thermodynamic stability of copper oxides, hydrides, and oxy-hydrides, relative to pure elements at the same temperature. The Δ*U* column presents the data recalculated from total energies of static ion configurations. The rest of thermodynamic data are derived using *ab initio* electronic structure calculations and phonon spectra calculations for the molecular species as well as for solid-state species. All the calculated data include an empirical correction to the ground-state energy of oxygen and hydrogen molecules (see text). Experimental data from Refs. /27, 15, 16/ are given in parenthesis.

Substance	Structure	Δ*U* kJ/mol	Δ*H*(0) kJ/mol	Δ*H*(298.15) kJ/mol	Δ*G*(298.15) kJ/mol
Cu_2O	cuprite	–164.4	–160.6	–161.9	–140.9
			(–168.9)	(–170.7)	(–147.9)
CuO	tenorite	–149.2	–146.0	–148.0	–144.7
			(–153.8)	(–156.1)	(–128.3)
CuH	wurtzite	+34.5	+39.5	+36.7	+50.9
				(+27.5)	(+54.0)
				(+55.1)	(+80.5)
CuH_2	fluorite	+141.8	+135.2	+132.5	+163.5
CuH_2	rutile	+97.5	+106.8	+100.7	+134.2
Cu_4H_2O	Cnf.1	+24.6	–	–	–
	Cnf.2	–22.8	–11.7	–17.7	+30.1
	Cnf.3	–38.1	–30.6	–35.6	+17.2

2.4 Conclusion about instability of copper oxy-hydride

Oxy-hydride Cu_4H_2O is found to be unstable even with respect to decomposition onto cuprous oxide and hydride,

$$Cu_4H_2O \rightarrow Cu_2O + 2CuH \qquad (2\text{-}4)$$

the enthalpy of the reaction is $\Delta H(0) = -53.0$ kJ/mol, $\Delta H(298.15) = -53.0$ kJ/mol, and the Gibbs free energy is $\Delta G(298.15) = -56.2$ kJ/mol (strongly exothermic reaction). Copper hydride is, in turn, unstable relative to pure substances, Cu(fcc) and H_2 (gas). According to this result, the possibility that an oxy-hydride of copper may form as a stable product of copper corrosion by pure water can be ruled out.

3 Copper hydroxide

The question of stability of copper hydroxide deserves a separate chapter. Partly this is because in recently published articles /33/ the product of corrosion of copper by water was identified as copper(I) hydroxide. Experimental information on the thermodynamic properties is available for charge-neutral molecular CuOH species in aqueous solution /10/, but not for copper(I) hydroxide in a solid form.

Because experimental data on the structure and stability of copper(I) hydroxide are lacking, our purpose is to derive these data using first-principles calculations of the electronic and phonon spectra. Technical details of our calculations are the same as those presented in Chapter 1.

3.1 CuOH molecule

We begin our analysis with the equilibrium geometry and vibrational frequencies of a single CuOH molecule (in these calculations ^{63}Cu, ^{16}O, and ^{1}H isotopes have been considered). The calculated interatomic distances are |Cu-O| = 3.34 bohr (1.77 Å) and |O-H| = 1.85 bohr (0.98 Å); the bond angle ∠Cu-O-H is 106.7°. The corresponding vibrational frequencies are 630 cm^{-1} (Cu-O stretching), 3,705 cm^{-1} (O-H stretching), and 820 cm^{-1} (Cu-O-H bending).

Formation energy of molecular CuOH, calculated with respect to pure elements in their standard states (crystalline fcc Cu and molecular O_2 and H_2) is positive: ΔU=+10.5 kJ/mol (for all the species in static ionic configurations) and $\Delta H(0)$=+21.2 kJ/mol (the energy of zero-point ionic motion is included).

3.2 The structure and stability of solid CuOH

The CuOH stoichiometry dictates the formal oxidation states of the ions to be Cu^{+}, O^{2-}, and H^{+}. Our preliminary calculations have shown that electronic structure (as well as total energy) of CuOH is extremely sensitive to the particular spatial arrangement of the atoms. This acute dependence of total energy on local co-ordination of ions puts an important topological constraint on the structure of solid CuOH, which considerably limits the number of configurations to be tried in the search for the ground-state structure of CuOH. In the present study, we adopted the following search strategy:

1. Pauling's rule should be obeyed for the relative coordination of cations and anions in any starting configuration, $\sum_i z_i / q_i = z_{Cu} + z_H - z_O / 2 = 0$, where z_i and q_i are the coordination number and the formal charge of ion i (coordination number is defined as the number of nearest-neighbor ions of the opposite charge).
2. It should be possible to completely partition any starting configuration onto individual Cu-O-H molecules. Here each '-' denotes a nearest neighbor bond. No Cu-O-Cu or H-O-H coordination is allowed.
3. The bond angle ∠Cu-O-H in a starting configuration should be close to that in the CuOH molecule. The symmetry of the structure is then set to zero and the structure is fully optimized (the lattice parameters and all the internal parameters).

The first setup that we tried was based on the face-centered cubic (fcc) sublattice of copper(I) cations. The oxygen anions and hydrogen cations (protons) were distributed in various ways among the interstitial sites. This approach produced highly-coordinated ions and was later found to yield very high energies as compared to low-coordinated structures of the second setup.

The second set of starting configurations was based on the body-centered cubic sublattice of oxygen anions (similar to cuprite). The cations were situated on the lines connecting two neighboring oxygen ions. Copper ions were put into the position mid-way between the oxygens (again like in cuprite), whereas the protons were shifted away from the midpoints, in order to facilitate proton disorder that is characteristic of low-pressure phases of ice.

There is a crystallographic relationship between the structures of Cu_2O (cuprite) and H_2O (ice). Chemical similarity between these two substances (both are monovalent oxides) becomes obvious if one considers a high-pressure phase of H_2O known as ice-X, which has the same cuprite crystal structure as Cu_2O. Upon lowering pressure, ice-X undergoes a proton-disordering transformation into ice-VII, upon which each proton moves away from the bond-center position close to one of the two O^{2-} ions, to form a molecular crystal comprised of H_2O molecules connected by hydrogen bonds.

Our search of stable conformations of CuOH molecules yielded structures that are intermediate between the cuprite Cu_2O and ice-VII H_2O. Two of such structures are shown in Figure 3-1. Both structures derive from a bcc sublattice of oxygen anions and exhibit cation coordinations characteristic of cuprite (two-fold Cu^+ coordination) and ice-VII (proton disorder involving hydrogen bonds). Because of this structural inheritance from the crystal structure of cuprite and ice, hereafter we refer to the derived structure of bulk CuOH as “cuprice”.

Like in the structure of ice, one can arrange the cations in CuOH in a variety of configurations similar to Configurations 1 and 2 shown in Figure 3-1. Provided that locally the cuprice structures are comprised by Cu_2OH coordination units, their energies are going to be nearly degenerate, as the chemical bonds in these structures are saturated and the bond angles are practically the same. Table 3-1 shows that this is indeed the case for Configurations 1 and 2. We note that other CuOH structures encountered in our search procedure were found to be much higher in energy than the cuprice structure. For example, CuOH in the crystal structure of lithium hydroxide (which is somewat similar to Configuration 2, but the metal cations are four-fold coordinated) is higher in energy than Configuration 2 by 58 kJ/mol.

The calculated phonon spectrum of CuOH (cuprice, Configuration 2) is presented in Figure 3-2. The mechanical stability of the structure is marginal; one notices a considerable softening of the lowest-lying acoustic branch along the Γ−Z direction. Vibrational modes of a CuOH molecule discussed in Section 3.1 allow for an easy interpretation of the peaks in the phonon DOS of solid CuOH. The peak at 3,400 cm^{-1} corresponds to the O-H bond stretch mode, the band near 900 cm^{-1} corresponds to the Cu-O-H bending mode, and the band below 600 cm^{-1} corresponds to the vibrations of a hydroxyl OH^- group as a whole.

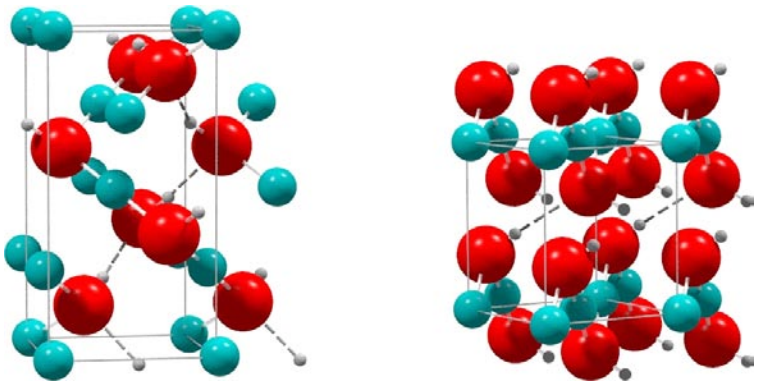

Figure 3-1. *Two stable configurations of bulk copper(I) hydroxide CuOH. Copper cations are shown as medium-size cyan balls, oxygen cations – as large red balls, and protons – as little gray balls. Sticks indicate primary chemical bonds. Broken lines show hydrogen bonds that form a helix in Configuration 1 (left) or a planar arrangement in Configuration 2 (right).*

Table 3-1. Thermodynamic stability of copper(I) oxide and hydroxide in comparison with that of water H_2O. The thermodynamic data for Cu_2O and CuOH have been derived using *ab initio* electronic structure calculations and phonon spectra calculations for the molecular and solid-state species. Calculated data include the empirical correction to the ground-state energy of oxygen and hydrogen molecules (see text). Experimental data for H_2O(liq.) are taken from Ref. /27/.

Substance	Structure	$\Delta H(0)$ kJ/mol	$\Delta H(298.15)$ kJ/mol	$\Delta G(298.15)$ kJ/mol
Cu_2O	cuprite	–160.6	–161.9	–140.9
CuOH	Conf. 1	–195.4	–199.8	–158.2
CuOH	Conf. 2	–196.5	–200.8	–160.8
H_2O	liquid	–	–285.8	–237.1

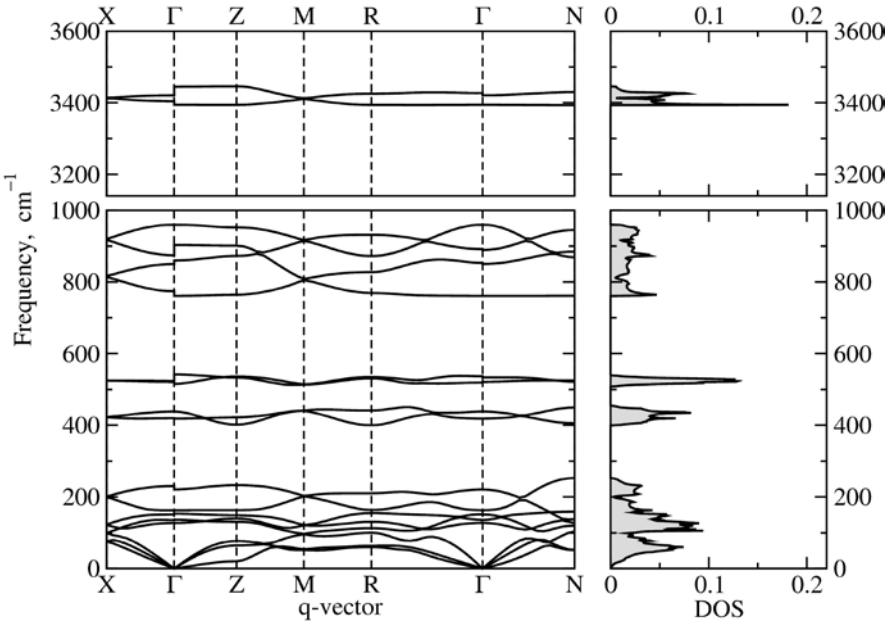

Figure 3-2. *Phonon spectrum and density of states (DOS) in copper(I) hydroxide, CuOH (Configuration 2), calculated at a molecular volume of 61.34 Å^3. Notations are similar to those in Figure 2-10.*

3.3 Summary of results for copper(I) hydroxide

Our calculations establish the fact that copper(I) hydroxide may be metastable in the solid form. We find that, if it exists, CuOH should be quite poorly crystalline since its most stable solid form (cuprice) allows for a high degree of intrinsic disorder similar to the proton disorder in ice. As follows from the presence of a bandgap in the electronic spectrum of CuOH (see Figure 3-3), the chemical bonds in the cuprice structure are saturated; the structure is additionally stabilized by hydrogen bonds. The variety of cuprice structures is found to be much more stable than the other candidate structures of CuH considered in our calculations. Therefore, we believe that our search has indeed yielded the most stable solid form of copper(I) hydroxide.

However, in spite of the very large negative enthalpy and free energy of formation calculated for cuprice (see Table 3-1), it is only metastable and should decompose onto cuprous oxide and water:

$$2CuOH \rightarrow Cu_2O + H_2O \qquad (3\text{-}1)$$

The enthalpy of the reaction is $\Delta H(298.15) = -46.1$ kJ/mol, and the Gibbs free energy is $\Delta G(298.15) = -56.4$ kJ/mol (a strongly exothermic reaction). The situation here is very similar to that in the case of copper(II) hydroxide, which is only metastable and decomposes spontaneously onto CuO and water. According to our results, copper(I) hydroxide cannot be a stable product of copper corrosion by pure water. However, the data on the electronic and vibrational spectra of various Cu-O-H compounds obtained in the course of this work may be useful for interpretation of experimental spectra of stable and metastable products of copper corrosion.

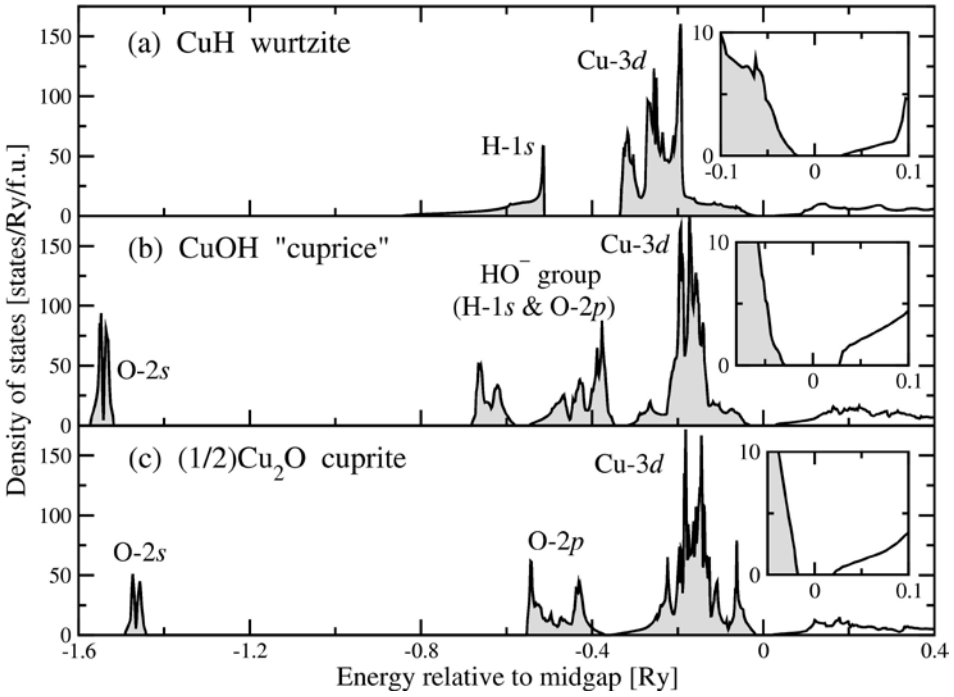

Figure 3-3. *Density of electron states (DOS) in copper(I) hydride CuH, hydroxide CuOH, and oxide Cu_2O. Labels near the DOS peaks indicate the predominant character of the corresponding states. The insert panels magnify the DOS at energies near the bandgap.*

Acknowledgments

Fruitful discussions with L. O. Werme, C. Lilja, E. I. Isaev, C. Ambrosch-Draxl, D. A. Andersson, O. Peil, and A. V. Ruban are acknowledged. The computations have been performed on the cluster Neolith at the National Supercomputer Center (NSC) in Linköping. The study has been financed by Svensk Kärnbränslehantering AB.

References

/1/ **Szakálos P, Hultquist G, Wikmark G, 2007.** Corrosion of copper by water, Electrochemical and Solid-State Letters 10, C63–C67.

/2/ **Hultquist G, 1986.** Hydrogen evolution in corrosion of copper in pure water, Corrosion Science 26, 173–176.

/3/ **Hultquist G, Chuah G K, Tan K L, 1989.** Comments on hydrogen evolution from the corrosion of pure copper, Corrosion Science 29, 1371–1377.

/4/ **Hultquist G, Chuah G K, Tan K L, 1990.** A SIMS study of reactions in the metal-oxygen-hydrogen-water system, Corrosion Science 31, 149–154.

/5/ **Simpson J P, Schenk R, 1987.** Short communication: Hydrogen evolution from corrosion of pure copper, Corrosion Science 27, 1365–1370.

/6/ **Eriksen T E, Ndalamba P, Grenthe I, 1989.** Short communication: On the corrosion of copper in pure water, Corrosion Science 29, 1241–1250.

/7/ **Pourbaix M, 1963.** Atlas d'Equilibres Electrochimique à 25°C (Gauthier-Villars, Paris).

/8/ **Mattsson E, 1980.** Corrosion of copper and brass: Practical experience and basic data, Br. Corros. J. London 15, 6–13.

/9/ **Beverskog B, Puigdomenech I, 1997.** Revised Pourbaix diagrams for copper at 25 to 300°C, J. Electrochem. Soc. 144, 3476–3483.

/10/ **Puigdomenech I, Taxén C, 2000.** Thermodynamic data for copper: Implications for the corrosion of copper under repository conditions. TR-00-13, Svensk Kärnbränslehantering AB.

/11/ **The Swedish Corrosion Institute and its Reference Group, 1978.** Copper as a Canister Material for Unprocessed Nuclear Waste – Evaluation with respect to Corrosion. KBS-TR-90, Svensk Kärnbränslehantering AB.

/12/ **The Swedish Corrosion Institute and its Reference Group, 1983.** Corrosion resistance of a copper canister for spent nuclear fuel, SKBF/KBSTR-83-24, Svensk Kärnbränslehantering AB.

/13/ **King F, Ahonen L, Taxén C, Vuorinen U, Werme L, 2001.** Copper corrosion under expected conditions in a deep geologic repository. TR-01-23, Svensk Kärnbränslehantering AB.

/14/ **Goedkoop J A, Andersen A F, 1955.** The crystal structure of copper hydride, Acta Cryst. 8, 118–119.

/15/ **Burtovyy R, Utzig E, Tkacz M, 2000.** Studies of the thermal decomposition of copper hydride, Thermochimica Acta 363, 157–163.

/16/ **Burtovyy R, WŃosewicz D, Czopnik A, Tkacz M, 2003.** Heat capacity of copper hydride, Thermochimica Acta 400, 121–129.

/17/ **Fitzsimons N P, Jones W, Herley P J, 1992.** Aspects of the synthesis of copper hydride and supported copper hydride, Catalysis Letters 15, 83–94.

/18/ **Fitzsimons N P, Jones W, Herley P J, 1995.** Studies of Copper Hydride: Part 1. – Synthesis and Solid-state Stability, J. Chem. Soc. Faraday Trans. 91, 713–718.

/19/ **Herley P J, Fitzsimons N P, Jones W, 1995.** Studies of Copper Hydride: Part 2. – Transmission Electron Microscopy, J. Chem. Soc. Faraday Trans. 91, 713–718.

/20/ **Hohenberg P, Kohn W, 1964.** Inhomogeneous electron gas, Phys. Rev. 136, B864–B871.

/21/ **Kohn W, Sham L J, 1965.** Self-consistent equations including exchange and correlation effects, Phys. Rev. 140, A1133–A1138.

/22/ **Vanderbilt D, 1990.** Soft self-consistent pseudopotentials in a generalized eigenvalue formalism, Phys. Rev. B 41 (Rapid Communications), 7892–7895.

/23/ **Baroni S, de Gironcoli S, Dal Corso A, Gianozzi P.** http://www.pwscf.org.

/24/ **S Baroni, de Gironcoli S, Dal Corso A, Gianozzi P, 2001.** Phonons and related crystal properties from density-functional perturbation theory, Rev. Mod. Phys. 73, 515–562.

/25/ **Giannozzi P, Baroni S, Bonini N, Calandra M, Car R, Cavazzoni C, Ceresoli D, Chiarotti G L, Cococcioni M, Dabo I, 2009.** QUANTUM ESPRESSO: a modular and open-source software project for quantum simulations of materials, J. Phys.: Condens. Matter 21, 395502 (2009); http://www.quantum-espresso.org.

/26/ **Irikura K K, 2007.** Experimental vibrational zero-point energies: Diatomic molecules, J. Phys. Chem. Ref. Data 36, 389–397.

/27/ **Chase M W, 1998.** NIST-JANAF Thermochemical Tables. Fourth Edition. Part II, Cr-Zr (American Institute of Physics, New York).

/28/ **Soon A, Todorova M, Delley B, Stampfl C, 2006.** Oxygen adsorption and stability of surface oxides on Cu(111): A first-principles investigation, Phys. Rev. B 73, 165424.

/29/ **Soon A, Todorova M, Delley B, Stampfl C, 2007.** Thermodynamic stability and structure of copper oxide surfaces: A first-principles investigation, Phys. Rev. B 75, 125420.

/30/ **Soon A, Todorova M, Delley B, Stampfl C, 2007.** Erratum: Thermodynamic stability and structure of copper oxide surfaces: A first-principles investigation, Phys. Rev. B 75, 129902(E).

/31/ **Soon A, Cui X -Y, Delley B, Wei S -H, Stampfl C, 2009.** Native defect-induced multifarious magnetism in nonstoichiometric cuprous oxide: First-principles study of bulk and surface properties of $Cu_{2-\delta}O$, Phys. Rev. B 79, 035205.

/32/ **Kurth S, Perdew J W, Blaha P, 1999.** Molecular and solid-state tests of density functional approximations: LSD, GGAs, and Meta-GGAs, Inlt. J. Quantum Chem. 75, 899–909.

/33/ **Hultquist G, Szakálos P, Graham M J, Belonoshko A B, Sproule G I, Gråsjö L, Dorogokupets P, Danilov B, AAstrup T, Wikmark G, Chuah G -K, Eriksson J -C, Rosengren A, 2009.** Water Corrodes Copper, Catal. Lett. 132, 311–316.

ISSN 1404-0344
CM Gruppen AB, Bromma, 2010